International Journal of Nanomedicine Dovepress

Open Access Full Text Article ORIGINAL RESEARCH

Dendritic Cell-Derived Exosomes Promote Tendon Healing and Regulate Macrophage Polarization in Preventing Tendinopathy

Rao Chen[1,2,*], Liya Ai[1,2,*], Jiying Zhang[1,3,4], Dong Jiang[1,3,4]

[1]Department of Sports Medicine, Peking University Third Hospital, Institute of Sports Medicine of Peking University, Beijing, 100191, People's Republic of China; [2]Department of Laboratory Animal Science, Peking University Health Science Center, Beijing, 100191, People's Republic of China; [3]Beijing Key Laboratory of Sports Injuries, Beijing, 100191, People's Republic of China; [4]Engineering Research Center of Sports Trauma Treatment Technology and Devices, Ministry of Education, Beijing, 100191, People's Republic of China

*These authors contributed equally to this work

Correspondence: Dong Jiang, Department of Sports Medicine, Peking University Third Hospital, Beijing, 100191, People's Republic of China, Email bysyjiangdong@126.com

Introduction: Tendon injuries present a significant challenge for independent repair, and can progress into tendinopathy over time, highlighting the importance of early intervention. Dendritic cell-derived exosomes (DEXs) has been shown to shift the polarization of M1 macrophages, the predominant inflammatory cells in the early stages of tendon injury. This study introduces a therapeutic approach that effectively manages inflammation while promoting regeneration in the treatment of tendinopathy.

Methods: The purification and characterization of DEXs were meticulously conducted. Experiments were carried out using an Achilles tendon rupture mouse model, with weekly DEXs treatment starting on postoperative day (POD) 4. In vitro, the function of DEXs was assessed by coculturing them with tendon stem/progenitor cells (TSPCs) in culture medium containing IL-1β. Tendon healing progress was evaluated using Sirius Red staining, Masson's trichrome staining, biomechanical testing, and immunofluorescence microscopy. The inflammatory microenvironment of injured tendons was evaluated using the Luminex procedure and flow cytometry analysis.

Results: DEXs treatment significantly enhanced tendon cell differentiation, promoted collagen type I synthesis, and inhibited collagen type III synthesis, thereby expediting tendon healing. Furthermore, DEXs treatment improved the inflammatory microenvironment by reducing multiple cytokines (IL-1β, IL-4, IL-6, TNF-α, and IFN-γ) and induced the conversion of M1 macrophages to M2 macrophages by activating the PI3K/AKT pathway.

Conclusion: DEXs demonstrated a potent ability to promote tendon healing while ameliorating the inflammatory microenvironment, suggesting their potential as a therapeutic approach to prevent the development of tendinopathy.

Keywords: dendritic cell-derived exosomes, macrophage polarization, tendinopathy, inflammatory microenvironment

Introduction

Tendons are soft, fibrous tissues that connect muscles to bones, playing a main role in transferring muscle-generated force to the skeleton and facilitating joint movement.[1] When tendons are damaged, their intrinsic hypocellularity and hypovascularity lead to slow and inefficient natural healing.[2] Chronic tendon injury, or tendinopathy, is a prevalent condition characterized by significant disability, pain and impaired performance, implicated in almost 30% of all musculoskeletal consultations.[3,4] Since the pathogenesis of tendinopathy is complicated, effective treatments for tendon injuries are lacking.[5,6] Studies have reported that multiple inflammatory factors are released after tendon injury, such as IL-1β, IL-6, TNF-α, MMP-13 and others.[7] The microenvironment around TSPCs may affect autologous proliferation and differentiation, thus influencing tendon healing.[8] In recent years, immunoregulatory therapy has garnered attention as an early stage therapy for preventing tendinopathy.[4]

Received: 28 February 2024
Accepted: 5 November 2024
Published: 13 November 2024

Graphical Abstract

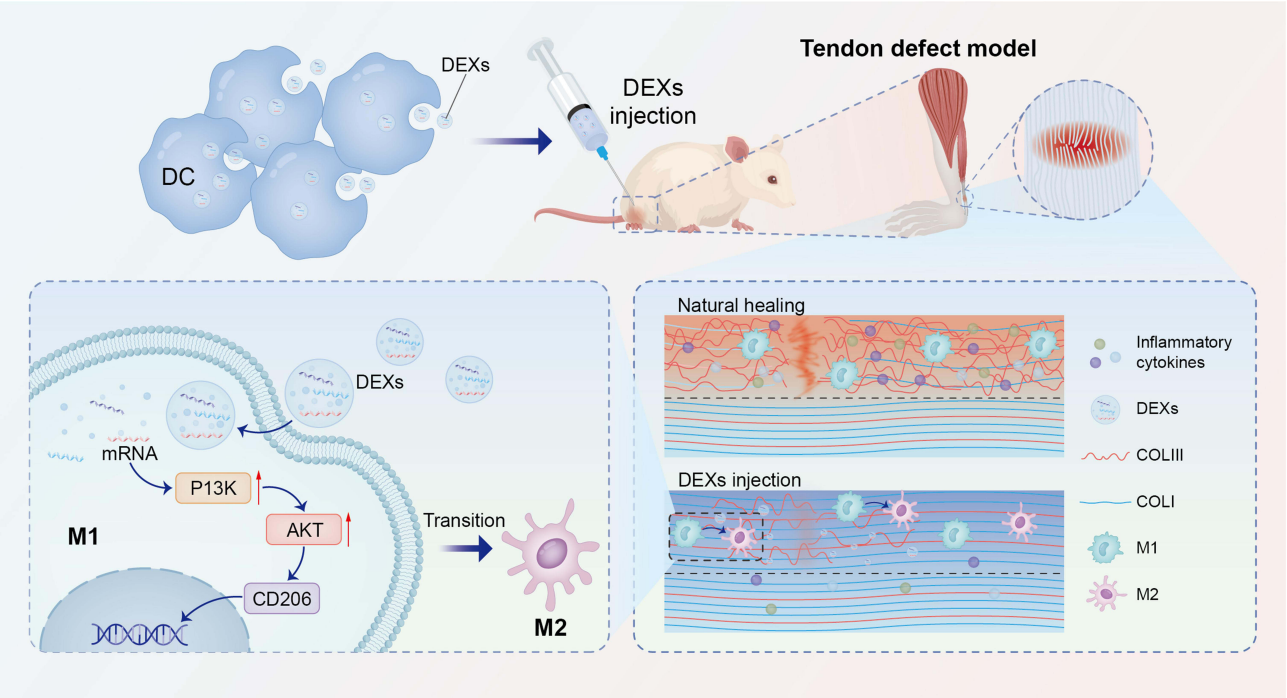

Type I collagen (COLI) is the predominant collagen in tendons, comprising approximately 90% of the total collagen content. This collagen is often replaced by other types following acute or chronic tendon injuries.[9] The inflammation caused by the injury can lead to hypoxia, which shifts matrix component synthesis towards a collagen type III (COLIII) profile.[10] Abnormal tendon repair after injury is considered one of the pathogenesis of ectopic ossification.[11] Without prompt treatment, tendon progenitor cells may undergo chondrogenic differentiation instead of forming tendon tissue.[12] Cytokines produced by leucocytes and tenocytes can also be expressed endogenously in response to trauma, and these agents are largely pro-inflammatory.[13] Therefore, early treatment and intervention are crucial to reduce damage and inflammation.

Our initial histology results indicated that both dendritic cells and macrophages, as intrinsic cells of the body, infiltrated the area surrounding the injured tendon, collectively influencing the local inflammatory microenvironment. Macrophages play crucial roles in both promoting and resolving inflammation, as well as in facilitating and moderating tissue repair. It has been demonstrated that macrophage-derived exosomes (EXOs) induce peritendinous fibrosis after tendon injury.[14] Dendritic cells (DCs) are a group of antigen-presenting cells, and their immunomodulatory function is closely tied to their cell state, typically categorized into immature DCs (imDCs) and mature DCs (mDCs). mDCs exhibit a high capacity to secrete inflammatory and immunostimulatory cytokines, while imDCs play regulatory and immunosuppressive roles that contribute to maintaining immune tolerance.[15] Similarly, immature dendritic cell-derived exosomes (imDEXs) display immunosuppressive effects due to their low content of major histocompatibility complex (MHC) molecules and costimulatory molecules.[16] To date, imDEXs and tolerogenic DEXs have been employed in immunotherapy for conditions such as rheumatoid arthritis and mouse heart transplantation.[17–19] However, the impact of imDEXs on the treatment and prevention of tendinopathy has not yet been investigated.

It have been demonstrated that DEXs can activate regulatory T (Treg) cells and shift M1 macrophages to reparative M2 macrophages.[20] In the tendon injury model, M1 macrophages predominate in the early stages.[21] Building on this, we aimed to investigate the inflammation regulatory mechanisms of DEXs after tendon injury, while also exploring their

potential to promote tendon healing and prevent the development of tendinopathy. In vitro experiments involved co-culturing TSPCs with DEXs in an IL-1β medium, and DEXs treatment was applied in a mouse Achilles tendon injury model. In the in vivo experiments, we analyzed levels of various inflammatory cytokines, tendon markers, extracellular matrix (ECM) markers, and collagen organization parameters. Our hypothesis was that modulating inflammatory responses post-injury could enhance tendon reconstruction, leading to a relatively higher concentration of COLI compared to COLIII. The findings presented in this study provide promising insights into a potential treatment method for preventing tendinopathy following tendon injury.

Materials and Methods

Isolation and Culture of TSPCs

The use of all experimental animals was approved by the Animal Experimentation Ethics Committee of the Institute of Sports Medicine, Peking University Third Hospital. All procedures involving BALB/c male mice (20 g, 7 weeks old) were conducted in accordance with the guidelines of the Institutional Animal Care and Use Committee. Achilles tendon samples were obtained from 5 wild-type (WT) BALB/c mice and cut into pieces using scissors. The samples were then subjected to digestion in a 37°C cell incubator using 0.2% type I collagenase combined with 0.08% dispase IV. The digestion process was halted within 1 hour using a culture medium [Dulbecco's modified Eagle's medium (DMEM), 10% fetal bovine serum (FBS), and 1% penicillin–streptomycin], then the cells were cultured with the same medium for 7 days. In the subsequent grouping experiments, TSPCs were divided into three groups: an untreated group, and two groups treated with IL-1β (10 ng/mL, Peprotech, 200–01B) for 24 hours. In the IL-1β treated groups, TSPCs were either left untreated or treated with DEXs (10 μg/mL, 72 hours) in 1 mL culture medium.[22]

Generation, Culture and Identification of Bone Marrow Dendritic Cells (BMDCs)

Mouse BMDCs were generated from bone marrow (BM) precursor cells cultured in RPMI 1640 supplemented with 10% FBS, L-glutamine (2 mm), non-essential amino acids (1X), sodium pyruvate (0.11 mg/mL), HEPES (10 nM), tissue culture-grade 2-mercaptoethanol (0.55 mm), penicillin (100 U/mL), streptomycin (100 μg/mL), GM-CSF (1000 U/mL, Roche), and IL-4 (500 U/mL, Roche), following established protocols. After four days of continuous culture at 37°C in a humidified chamber with 5% CO_2, BMDCs were maintained in the culture medium with 10% EXO-free FBS during the final 48 hours. EXO-free FBS was prepared by subjecting FBS to 100,000 g centrifugation for 18 hours at 4 °C, followed by filtration through 0.22 μm-pore filters. For DEXs isolation, the cultured BMDCs were categorized into unstimulated imDC. mDC were stimulated with Lipopolysaccharide (LPS) for 48 hours and then stained with FITC-CD11b, PE-CD86, PE-Cy5.5 CD80 antibodies (Abs) for flow cytometry analysis.

Isolation and Characterization of DEXs

DEXs were purified from the culture supernatants (200 mL) of BMDCs following the guidelines of the International Society of Extracellular Vesicles. DC culture supernatants were successively centrifuged at 2000 g for 20 min and 10,000 g for 30 min, both at 4 °C. The remaining supernatants were concentrated by ultrafiltration on sterile Ultra-15 centrifugal filters (Amicon®, 30KDa, 2800 g, 4 °C). The concentrated supernatants were then adjusted to a volume of 66 mL with PBS, filtered through 0.22 μm-pore filters, and centrifuged at 110,000 g for 90 min at 4 °C. The 110,000 g pellets from the 110,000 g spin were resuspended in 1 mL, and stored at −80 °C for DEXs experiments. Western blotting was then performed to identify surface makers on the DEXs, including CD81 (Santa Cruz, sc-166029), HSP70 (Santa Cruz, sc-66048), CD9 (CST, 13174) and Calnexin (Abcam, ab22595). A transmission electron microscope (TEM, JEOL, JEM-1400) was used to access particle morphology. DEXs (10 μL) were dropped onto a copper grid, stained with 2% uranyl acetate solution for 1 min, and images were obtained using TEM with a 20,000 × magnification. The particle size distributions of isolated DEXs suspended in PBS were also determined using a Nanosight NS300 (Malvern, UK). To track the DEXs, the suspension was mixed with CellTracker™ CM-Dil dye (Invitrogen™, 0.1 μg/μL) at 37°C for 5 min,

followed by incubation on ice for 20 min. The mixture was then purified using an Amicon centrifugal filter at 14,000 g for 5 min to remove the unincorporated dye.

Nano Flow Cytometer (nFCM) Analysis

For nFCM analysis, 5 μL of APC-conjugated Abs against CD9, CD63, and CD81 were respectively added to three different Eppendorf tubes, each containing 5 μL of DEXs sample. The mixtures were incubated at room temperature for 1 hour. Unbound antibodies were then washed twice with 1 mL of PBS by ultracentrifugation at 100,000 g for 17 minutes at 4°C. The resulting pellets were resuspended in 100 μL of PBS and analyzed using a nFCM (Apogee, Micro-PLUS GxP). An unstained DEXs sample (5 μL), diluted 20-fold with PBS, was used as a control for the nFCM analysis. Data were analyzed using FlowJo V10.6.2 software (TreeStar, Ashland, OR).

Animal Experiments and Tendon Injury Model Construction

Animal experiments were conducted with approval by the Peking University Health Science Center Ethics Committee and in strict accordance with the guidelines of the Institutional Animal Care and Use Committee of Laboratory Animals. The tendon injury model referred was constructed following the Liu et al's protocol.[23] Bilateral Achilles tendons were injected with type I collagenase (0.1 mg per leg; Gibco, 17100017). Subsequently, we used a 25-gauge needle to prick the tendon at five different points.[20] DEXs (1×10^9 nanoparticles) were injected subcutaneously and bilaterally (between Achilles tendon and skin) at POD 4,[8] with repeated injections weekly for three times, Achilles's tendon samples were collected at POD 32 and POD 46 for relative examinations. Another group were injected with same volume of PBS at the same time points and corresponding injury sites, and set as the control group; A normal group of animals without injury, was set as the blank control (BC) group. Combined with DEXs treatment, another group was treated with LY294002, a PI3K/AKT pathway inhibitor, at a concentration of 10 mg/kg via intraperitoneal injection twice per week for 4 weeks.

Hot Plate Test

The hot plate test was used to assess the pain response in the Achilles tendons of mice on POD 32 and 46. Both the Control and DEXs groups consisted of 3 mice each. Mice with tendon injuries were placed on a hot plate set to 55°C. The first response time of the hindlimbs, such as licking or jumping, was recorded. To prevent injury, mice were removed from the plate if their latency in responding to the thermal stimulus exceeded 30 seconds.

Tissue Specimen Processing and Microscopy Imaging

Tissue specimens collected at POD 32 and POD 46 were fixed in 4% paraformaldehyde, washed with running water, dehydrated in a graded ethanol series, vitrified with dimethylbenzene, and embedded in paraffin. Paraffin sections (7 μm) were deparaffinized in xylene, hydrated with a gradient of ethanol, and stained with a standard Sirius Red staining kit (Solarbio), or Masson's trichrome staining procedures. The polarization microscope was utilized to capture images of COLI and COLIII of Sirius Red staining sections.

Tissue specimens collected at POD 32 were examined by immunofluorescence staining, sections were incubated with 0.4% pepsin for 30 min and permeabilized with 0.2% Triton X-100 in PBS for 15 min. The sections were then blocked with 5% goat serum, incubated with the primary antibody at 4°C overnight, rinsed with PBS, and incubated with the secondary antibody at room temperature for 1 hour. The primary antibodies used in this research included rabbit anti-collagen I (Abcam, ab270993; 1:100 dilution), rabbit anti-collagen III (Abcam, ab7778; 1:100 dilution), rabbit anti-CD68 (Abcam, ab283654; 1:100 dilution), APC-conjugated anti-CD11b antibody (Biolegend, 101212, 1:50 dilution), FITC-conjugated anti-CD11c (Biolegend, 117305; 1:50 dilution), PE-conjugated anti-CD207 antibody (Biolegend, 144207, 1:50 dilution). All slides were treated with DAPI for nuclear staining. Images of the slides were captured with a confocal microscope (Zeiss, China) and analyzed for fluorescence intensity using Zen 3.3 (blue edition) software provided by Zeiss.

Quantitative Real-Time PCR (qRT-PCR)

Total RNA was extracted using TRIzol reagent (Invitrogen), and complementary DNA was synthesized with a reverse transcription system (ThermoFisher) following the manufacturer's instructions. Quantitative real-time polymerase chain

Table 1 Primers Sequences Used for RT-qPCR

Primer name	Sequence (5'-3')	Species
CCL27-Forward	TGGAAGCGGAGGAGGAGAT	Mouse
CCL27-Reverse	TAATGCACCGGCTGTCTGT	Mouse
CXCL10-Forward	ATGATGACACGACAGATGACTC	Mouse
CXCL10-Reverse	AGGCTCGCAGGGATGATTTC	Mouse
mActb247-Forward	GTACCACCATGTACCCAGGC	Mouse
mActb247-Reverse	AACGCAGCTCAGTAACAGTCC	Mouse
Scx-Forward	ACCGCACCAACAGCGTGAACAC	Mouse
Scx-Reverse	CAGCACATTGCCCAGGTGAGAA	Mouse
Mkx-Forward	TGGTTTCCTGGACAATCCACA	Mouse
Mkx-Reverse	CGCTTATGCCTTACCTTCCCTC	Mouse
Tnmd-Forward	ACACTTCTGGCCCGAGGTAT	Mouse
Tnmd-Reverse	GACTTCCAATGTTTCATCAGTGC	Mouse
TNC-Forward	TGAGACCTGACACGGAGTATG	Mouse
TNC-Reverse	TGAGACACGGCGGAGATTC	Mouse
Col1a1-Forward	TAAGGGTCCCCAATGGTGAGA	Mouse
Col1a1-Reverse	GGGTCCCTCGACTCCTACAT	Mouse
Col3a1-Forward	AGCCACCTTGGTCAGTCCTA	Mouse
Col3a1-Reverse	GTGTAGAAGGCTGTGGGCAT	Mouse

reaction (qRT-PCR) was conducted using the iQ5 optical system software (Bio-Rad) and FastStart Universal SYBR Green Master Mix (Roche, Basel, Switzerland) for mRNA quantitation of all indicated genes. Relative expression levels were calculated using the $2^{-\Delta\Delta Ct}$ method and normalized to β-actin. The quantitative RT-PCR primer sequences are listed in following Table 1.

Scanning Electron Microscopy (SEM)

SEM was employed to assess the collagen arrangement in the injured Achilles tendon on POD 7 without DEXs treatment, with a normal Achilles tendon serving as a control. Tendon tissues were fixed with 2.5% (v/v) glutaraldehyde in PBS for 24 hours, dehydrated using a graded alcohol series, and thoroughly dried using a vacuum drying apparatus. The dried samples were sputter-coated with gold-palladium and observed using a JSM-7900F microscope (JEOL Ltd, Japan). The images showing the cross section of the tendon were taken with a 20,000 magnification.

In vivo Fluorescence Imaging and Analysis

At 24 hours, 48 hours, and 72 hours after the subcutaneous injection of CM-dil-labeled DEXs, mice were anesthetized with inhaled isoflurane. Fluorescence images of the mice were captured using the Interactive Video Information System (IVIS) Spectrum (PerkinElmer). The distribution of DEXs in the Achilles tendon was quantified by calculating the fluorescence intensity of the Region of Interest (ROI).

Biomechanical Testing

Biomechanical Testing was performed at POD 32. The Achilles tendons were immersed in cold PBS to prevent drying, then placed in Eppendorf tubes on ice for biomechanical testing. Using a metal clamping device attached to a tensile tester (Care Measure & Control, IPBF-300), the samples were securely fastened. The clamps were positioned and fixed accordingly (refer to Figure S1A). Upon preconditioning the tendons with a force of 1N, the testing commenced. The displacement rate was set to 10 mm/min. Force-displacement curves were recorded using CAREUM1.0.3 software, with failure defined as the maximum load following the initial decrease in load tension.

RNA Sequencing

Tendon tissues from mice models were ground in RNA later (Invitrogen) to prevent RNA degradation. After verification of the RNA integrity, the extracted RNA was reverse-transcribed to generate a cDNA library for subsequent sequencing.

Luminex Procedure

Protein supernatant was obtained after tissue cleavage, and the BCA kit was utilized to determine the concentration. Subsequently, the final protein concentration of loading samples was uniformly set at 1.8 μg/μL. For the multiplex assays, we followed the procedures outlined in the mouse chemokine panel 31-plex kit (Bio-rad, 12009159). 50 μL of beads were added to each well for each bead set. Then, 25 μL of samples and 50 μL of detection Abs were added to the microspheres and incubated for 1 hour on a covered plate shaker at approximately 800 rpm. Following incubation, excess samples were removed by two washes of 150 μL of PBS-0.5% Tween-20. The plate was washed and supplemented with 50 μL of streptavidin-PE at a concentration of 20 μg/mL, and incubated for 30 minutes. The bead reporter fluorescence, expressed as the median fluorescence intensity (MFI), was determined with Luminex X-200 and analyzed using the Milliplex Analyst software 5.1.

Generation and Culture of Macrophages

Mouse bone-marrow-derived macrophages (BMDMs) were generated from BM precursor cells cultured in RPMI 1640 supplemented with 10% FBS, L-glutamine (2 mm), non-essential amino acids (1X), sodium pyruvate (0.11 mg/mL), HEPES (10 nM), tissue culture-grade 2-mercaptoethanol (0.55 mm), penicillin (100 U/mL), streptomycin (100 μg/mL), and macrophage colony-stimulating factor (M-CSF, 20 ng/mL; MCE, HY7085A) for a period of 7 days. The BMDMs were induced into M1 macrophages by treating them with interferon-γ (IFN-γ, 20 ng/mL, Peprotech) and lipopolysaccharide (LPS, 100 μg/mL, Sigma–Aldrich) for 24 hours. In the subsequent grouping experiments, the M1 macrophages were divided into three groups including an untreated group, a group treated with DEXs (40 μg/mL) for 4 days,[20] and a group treated with LY294002 (10 μM/mL, MCE) combined with DEXs (40 μg/mL) for 4 days.

Flow Cytometry Analysis

Achilles tendon samples collected at POD 32 were dissected using scissors, digested in 0.4% type I collagenase at 37°C for 1 hour, and the digestion was halted with culture medium. Single cells were then filtered through 70 μm cell strainers and rinsed with staining buffer. Cells were pre-incubated with CD16/32 antibody to minimize nonspecific antibody (Ab) binding and subsequently stained with BV421-CD68 Ab, APC-CD11b Ab, PE-CD86 Ab, or another set of APC-CD4, FITC-CD25, PE-CD152 Abs, together with fixable viability dye (FVD) for 30 minutes at 4°C. For intracellular staining, fixation was carried out using 4% PFA, and cells were rinsed twice with intracellular staining wash buffer. Subsequently, cells were stained with FITC-CD206, and PE-Cy7-CD301 Abs. Flow cytometry analysis was performed using a FACS machine (Beckman, CytoFLEX S), and data were analyzed using FlowJo V10.6.2 software (TreeStar, Ashland, OR).

Western Blotting (WB)

Achilles tendon samples collected at POD 32 were dissected using scissors, homogenized with a magnetic grinding instrument, and lysed with RIPA buffer supplemented with phosphatase inhibitors (Thermo Scientific™, 89,900). The resulting homogenate was then centrifuged at 14,000 g for 10 minutes at 4°C, and the pellet was removed. Protein quantification of the supernatant was performed.

For macrophage cultures, after removal of the culture medium, cells were washed with PBS and scraped off with cell scrapers. The cells were then lysed by adding RIPA buffer to the Eppendorf tubes and placed on ice for at least 30 minutes. Following cell lysis, the mixture was centrifuged at 14,000 g for 10 minutes at 4°C to obtain proteins in the supernatant.

The Western blot system was established using the Bio-Rad Bis-Tris Gel system according to the manufacturer's instructions. 5% BSA buffer was used for blocking at room temperature for 1 hour. The primary antibody was incubated at 4°C overnight, followed by washing and incubation with a secondary antibody marked by horseradish peroxidase for

1 hour at room temperature. Finally, the images were captured after the PVDF membranes were exposed to far-infrared rays. Adjustment of Western blot images was performed using Image Lab software. The antibodies used in the study were purchased from Cell Signaling Technology: rabbit anti-PI3 Kinase p110α (C73F8), rabbit anti-Phospho-PI3 Kinase p85 (Tyr458)/p55 (Tyr199), rabbit Phospho-Akt (D9E), rabbit anti-Akt (C67E7).

DEXs Uptake by TSPCs and Macrophages

TSPCs and macrophages were cultured in confocal wells, and 10 μL CM-dil-labeled DEXs were added to the cell medium. After co-culturing for 24 hours at 37°C, cells were fixed with PFA for 20 min, washed, stained with Alexa Fluor 488 Phalloidin (Invitrogen), then stained with DAPI, and examined using a confocal microscope (Zeiss, China).

Statistical Analysis

Quantitative data were expressed as means ± SD. Student's *t*-test was conducted to assess the presence of statistical differences between groups. P values less than 0.05 were considered statistically significant. The significance levels are denoted as *P < 0.05, **P < 0.01, ***P < 0.001, and ****P < 0.0001.

Results

Characterization of DCs and DEXs

Flow cytometric analysis was performed to identify the phenotype of DCs. The cultured BMDCs used for DEXs isolation were identified as imDCs, characterized by low expression of CD86 and CD80 (Figure 1A). WB analysis, nanoparticle tracking analysis (NTA), and TEM were employed to identify particles derived from BMDCs. WB analysis revealed that these vesicles were positive for exosome-specific markers HSP70, CD81, and CD9, while negative for the marker calnexin (Figure 1B). TEM and NTA demonstrated abundant DEXs with a diameter ranging from 70 to 150 nm (Figure 1C and D). In contrast, lysed DEXs showed no normal vesicle shape on TEM (Figure 1E). These findings were consistent with previous reports, confirming that the extracted vesicles were indeed DEXs. nFCM was performed to assess the purity of the extracted DEXs, the results showed that the expression quantity of CD9, CD63, and CD81 was 30.2%, 28.3% and 32.6%, respectively (Figure 1F).

DEXs Treatment of TSPCs in vitro

We subsequently established that DEXs were effectively captured by TSPCs, as illustrated in Figure 2A. To simulate an inflammatory microenvironment, IL-1β was introduced to the TSPCs, resulting in elevated concentrations of chemokines (CXCL10 and CCL27) and the inflammatory cytokine IL-6 of the TSPCs (Figure 2C and D). Concurrently, IL-1β treatment caused a decrease in the expression of COLI (Figure 2B). Upon treatment with DEXs, TSPCs exhibited higher expression of tendon markers, including Scx, Mkx, and Tnmd, as evidenced (Figure 2E). Notably, this treatment also increased COLI expression while reducing COLIII levels (Figure 2B).

DEXs Treatment of a Mouse Model of Tendinopathy

The tendon injury model was constructed following the procedures outlined by Liu et al. DEXs were administered subcutaneously to the injured site on POD 4, followed by weekly injections of the same dose for three weeks to help the tendons traversing the inflammatory window. Mice were euthanized at 4 and 6 weeks (POD 32 and POD 46) after initial DEXs injection (Figure 3A).

SEM observations revealed a severe breakdown of the collagen matrix and a loss of well-aligned collagen fibers in tendon injuries (Figure 3B), which are characteristic features of tendinopathy.[2] After four weeks of treatment, compared to the control group, the tendon surface in the DEXs-treated group appeared smooth, with no obvious tendon ruptures observed (Figure S1B). A higher ratio of COLI-to-COLIII ratio in the DEXs-treated group at both POD 32 and POD 46 were demonstrated by Sirius Red staining under a polarization microscope (Figure 3C). Masson's trichrome staining revealed morphological differences between the DEXs-treated group and control groups, with more mature (stained red) and less immature (stained blue) collagen in the DEXs-treated tendons (Figure 3D).[24] Immunofluorescence staining and

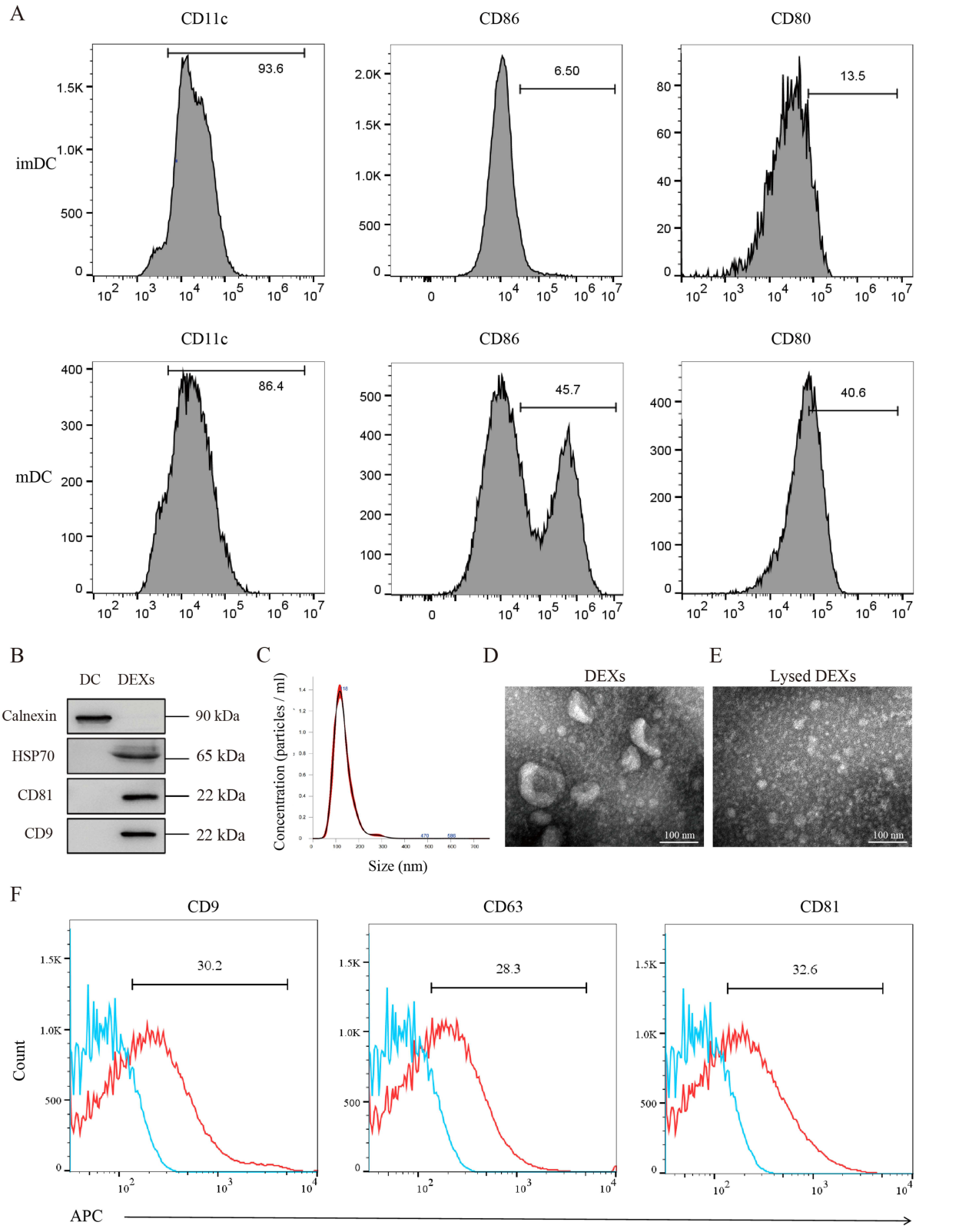

Figure 1 Characterization of DCs and DEXs. (**A**) Flow cytometry analysis of DC subsets (imDC and mDC) is presented in histograms as representative data. (**B**) EXO surface markers were detected using WB. (**C**) Nanoparticle tracking analysis was performed on DEXs, revealing a mode diameter of 118 nm. (**D**) The morphology of DEXs was observed through TEM, indicated by white arrows. (**E**) The image of lysed DEXs observed through TEM. (**F**) The expression levels of CD9, CD63, and CD81 were measured using nFCM.

Abbreviations: DCs, dendritic cells; DEXs, Dendritic cell-derived exosomes; imDC, immature dendritic cells; mDC, mature dendritic cells; EXO, exosome; WB, Western blotting; HSP 70, heat shock protein 70; TEM, transmission electron microscopy; nFCM, nano flow cytometer.

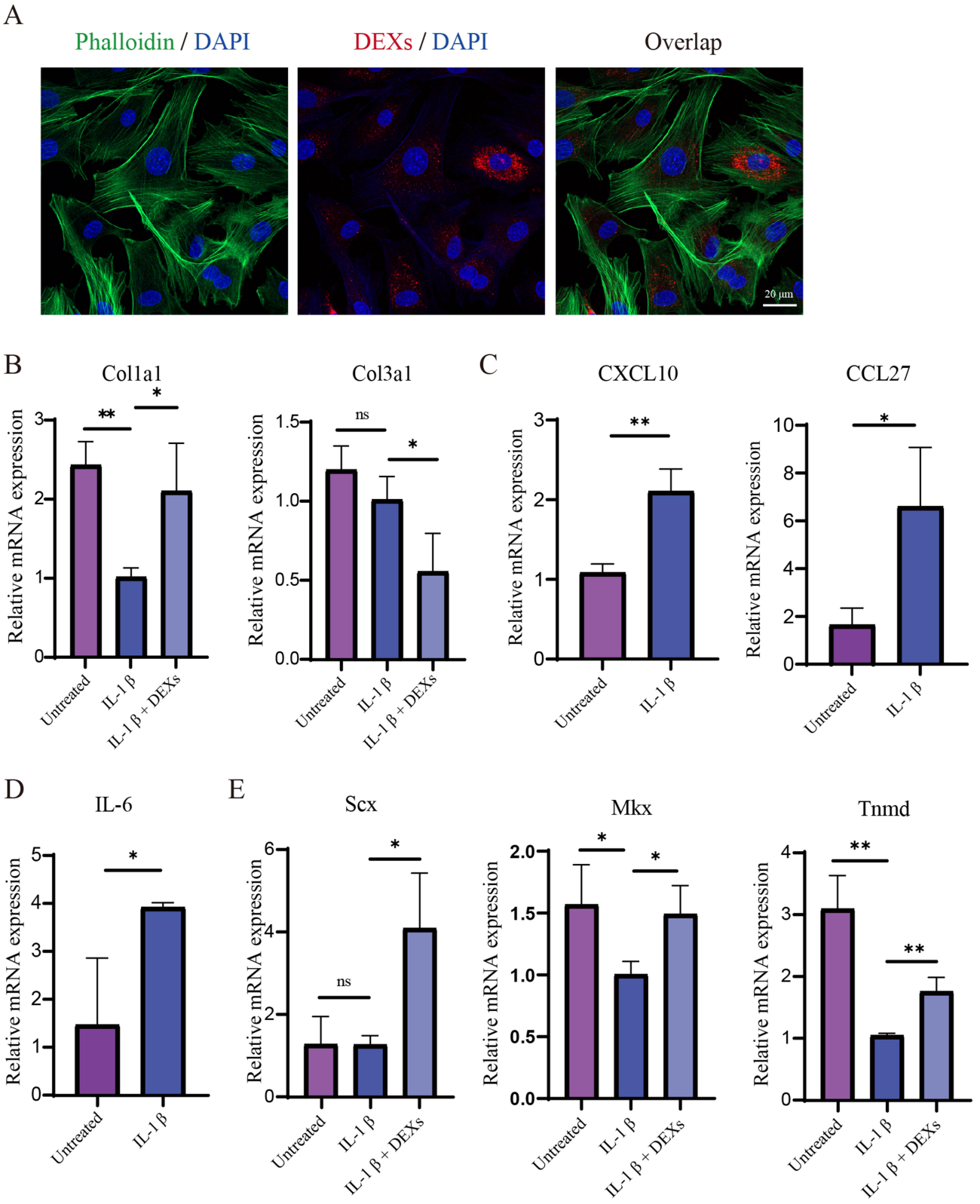

Figure 2 In vitro assessment of the stimulatory effect of DEXs on TSPCs in inflammatory mediators. (**A**) Investigation of CM-dil-labeled DEXs uptake by TSPCs using confocal microscopy. Scale bar: 20 μm. (**B–D**) Detection of the relative mRNA expression of Col1a1, Col3a1, CXCL10, CCL27 and IL-6 by qRT-PCR (n=3). (**E**) Assessment of the relative mRNA expression of tendon markers in TSPCs by qRT-PCR (n=3). *P < 0.05, **P < 0.01.

Abbreviations: TSPCs, tendon stem/progenitor cells; DAPI, diaminidine phenyl indole; CXCL10, C-X-C motif ligand 10; CCL27, C-C motif ligand 27; IL-6, interleukin 6; Scx, scleraxis; Mkx, mohawk; Tnmd, tenomodulin.

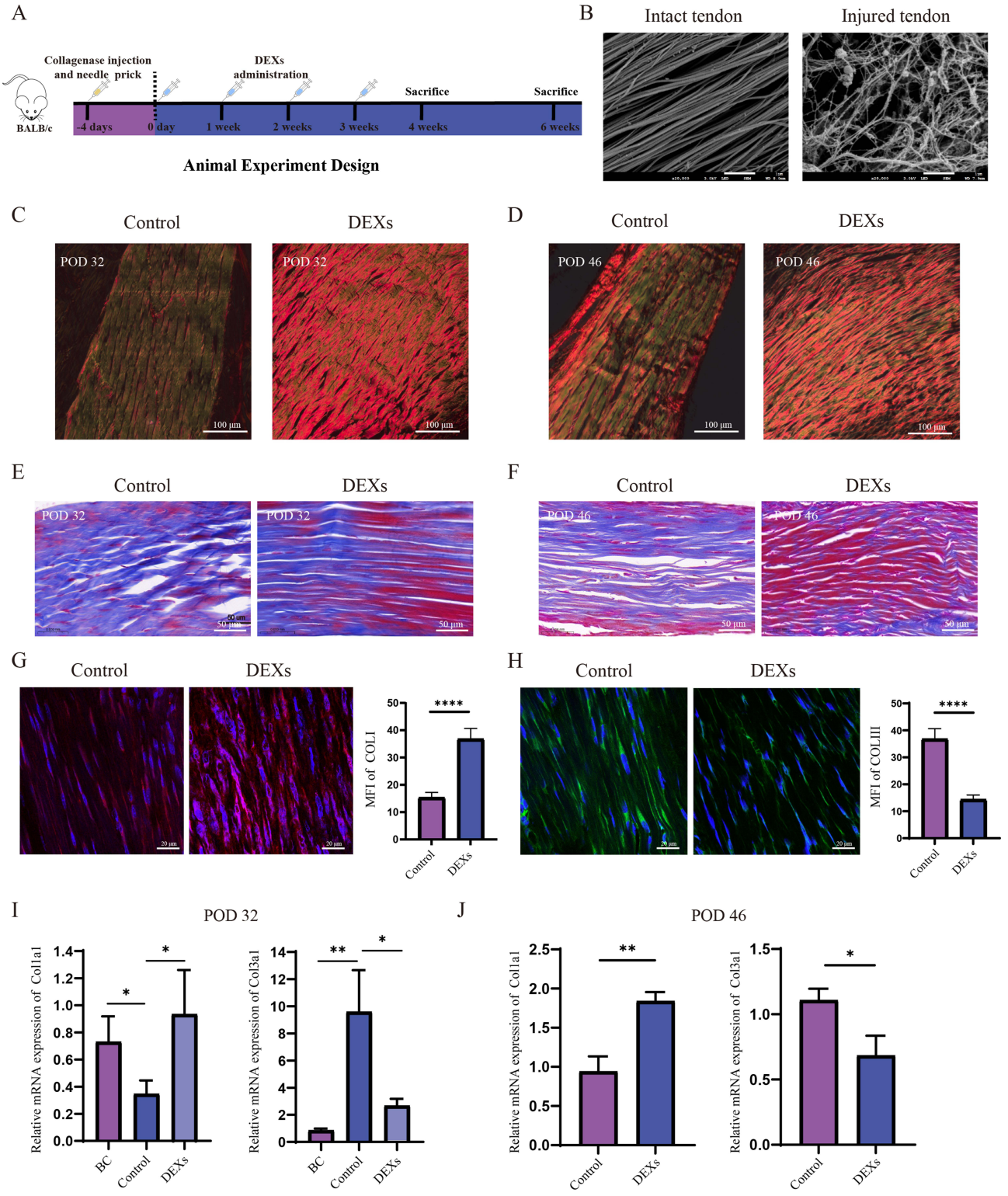

Figure 3 In vivo assessment of therapeutic effect of DEXs on tendon repair in a mouse model of tendinopathy. (**A**) Animal experiment design. (**B**) SEM images of intact and injured tendon. (**C** and **D**) Representative images of Sirius Red staining in the control and DEXs-treated groups at POD 32 and POD 46. (**E** and **F**) Representative Masson's trichrome staining images in the control and DEXs- treated groups at POD 32 and POD 46. (**G** and **H**) Immunofluorescence staining for COLI and COLIII (n=6). (**I** and **J**) Detection of the relative mRNA expression of Col1a1 and Col3a1 in injured Achilles tendon at POD 32 and POD 46 by qRT-PCR (n=3). *P < 0.05, **P < 0.01, ****P < 0.0001.
Abbreviations: SEM, scanning electron microscopy; COLI, collagen type I; COLIII, collagen type III; qRT-PCR, quantitative Real-time PCR; BC, blank control.

qRT-PCR results further confirmed that DEXs treatment promoted the expression of COLI and inhibited the expression of COLIII (Figure 3F and G). These findings collectively suggest that DEXs can enhance normal collagen organization and tendon healing.

Immunofluorescence staining revealed the infiltration of DCs and macrophages into the injured tendon, impacting the tendon repair process as innate immune cells. These cells may also serve as sources of inflammatory cytokines or chemokines (Figure 4A and B). Subcutaneously injected DEXs were captured by the injured tendon and retained at the site, exhibiting a daily gradual decline (Figure 4C and D). At the time points when the mice were sacrificed, DEXs administration significantly reduced pain sensitivity in tendinopathy mice, as measured by the response time in hot plate tests (Figure 4E). Additionally, CCL2, a marker of neuropathic pain,[25] was significantly lower in the DEXs-treated group. The maximum load that Achilles tendon could withstand in the control group decreased after injuries, but was excellently restored excellently after four times of DEXs treatment (Figure 4G). The tensile modulus of DEXs-treated group was also significantly higher than that of the control group (Figure 4H). Furthermore, DEXs treatment promoted the expression of tendon formation markers at both POD 32 and POD 46, as confirmed by qRT-PCR, including Scx, Mkx, and Tnmd (Figure 4I). These results indicate that DEXs treatment promotes tendon healing and the restoration of biomechanical properties.

RNA Sequencing of Injured Achilles Tendon

In our RNA sequencing analysis of the injured Achilles tendon, we utilized the control group as a reference and identified 461 down-regulated genes and 141 up-regulated genes in the DEXs group (fold change ≥ 2; q value < 0.05) (Figure 5A). Subsequent comparisons of gene expression differences between the control and DEXs groups (Figure 5B), along with gene ontology (GO) biological process analysis (Figure 5C), revealed that DEXs treatment facilitated tendon cell differentiation, collagen fibril organization, and tendon formation. Additionally, it down-regulated genes associated with collagen degradation and ossification. Kyoto Encyclopedia of Genes and Genomes (KEGG) statistics demonstrated that DEXs treatment affected PI3K/AKT, JAK-STAT, and mTOR signaling pathways (Figure 5D). Notably, the PI3K/AKT pathway exhibited the best Q value. The heatmap presents the relative levels of key genes in the PI3K/AKT signaling pathway, including IL-7R, dit4, syk, Itgb7, and Tnc. Furthermore, gene set enrichment analysis (GSEA) results indicated that DEXs treatment upregulated the AKT signaling pathway and fostered tolerant macrophages (Figure 5E). We validated the promotion of tendon formation by DEXs treatment at the protein level with WB for AKT, p-AKT, PI3K and p-PI3K (Figure 5F).

The Integrity of DEXs Affects Their Ability to Regulate the Peritendinous Inflammatory Microenvironment

Lysed DEXs were also administered to evaluate the effect of vesicle integrity on their therapeutic effectiveness in tendinopathy treatment. DEXs can induce T cells to differentiate into Treg cells, which possess strong immunomodulatory functions. Flow cytometry analysis of the inflammatory cells infiltrating the Achilles tendons revealed a higher ratio of Treg cells in the DEXs-treated group compared to the control or lysed DEXs-treated groups (Figure 6A and B). The conversion of M1 macrophages to M2 macrophages is a critical aspect of injury repair and immune tolerance. Building on insights from GSEA results, we conducted experiments to investigate the impact of DEXs therapy on macrophage polarization. In vivo, within the gated $CD11b^+$ live cell population, flow cytometry analysis revealed a significant decrease in the ratio of $CD68^+CD86^+$ cells (M1 macrophages) and a significant increase in the ratio of $CD206^+CD301^+$ cells (M2 macrophages) after DEXs treatment.[26] However, no significant difference was observed between the DEXs-treated and lysed DEXs-treated groups (Figure 6C–). These findings indicate that DEXs effectively promote the polarization of infiltrated macrophages from M1 to M2. Additionally, Luminex analysis was used to detect the peritendinous inflammatory microenvironment. Compared to the control group, DEXs treatment resulted in the downregulation of multiple inflammatory cytokines and chemokines, including IL-1β, IL-4, IL-6, TNF-α, IFN-γ, CCL27, and CXCL10 (Figure 4F and G). However, no statistically significant differences were observed between the control and lysed DEXs-treated groups, except for the chemokine CXCL10.

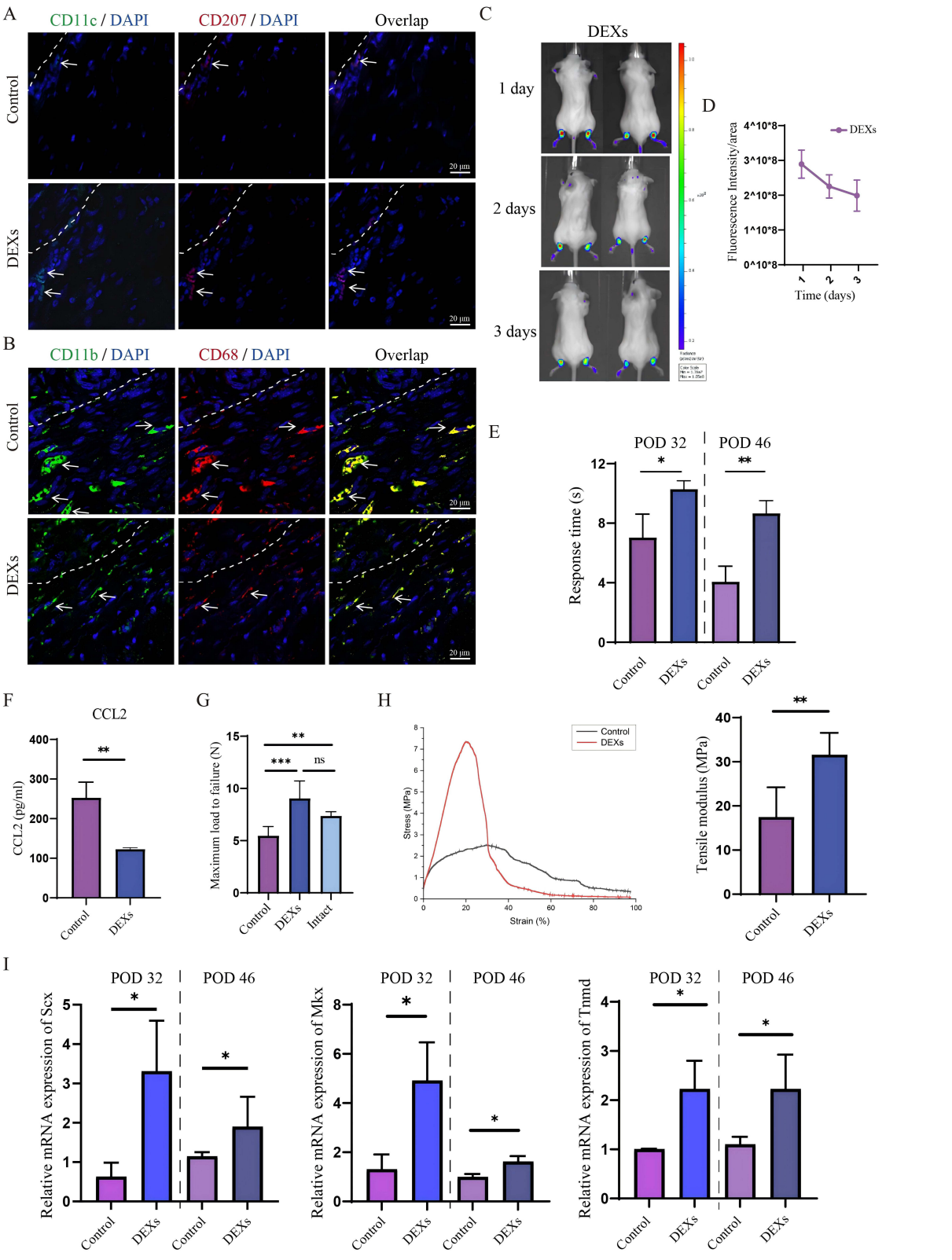

Figure 4 In vivo assessment of immunomodulatory effects of DEXs on the inflammatory microenvironment in a mouse model of tendinopathy. (**A**) Immunofluorescence staining for CD11c and CD207. Scale bar: 20 μm. (**B**) Immunofluorescence staining for CD11b and CD68. Scale bar: 20 μm. (**C**) In vivo fluorescence images of injured Achilles tendon after subcutaneous injection of CM-dil-DEXs. (**D**) Changes in fluorescence intensity per area (n=4). (**E**) Pain response time when mice were placed on a 55°C hot plate at 4 weeks (POD 32) and 6 weeks (POD 46) after DEXs treatment (n=3). (**F**) The CCL2 content of the injured tendon assessed by Luminex (n=3). (**G**) The maximum load that could be beared by the tendon among different groups (n=3). (**H**) Representative stress-strain curves and tensile modulus (n=3). (**I**) Assessment of the relative mRNA expression of tendon markers in injured Achilles tendons at POD 32 and POD 46 by qRT-PCR (n=3). *P < 0.05, **P < 0.01, ***P < 0.001.
Abbreviations: ns, no significance; CCL2, C-C motif ligand 2.

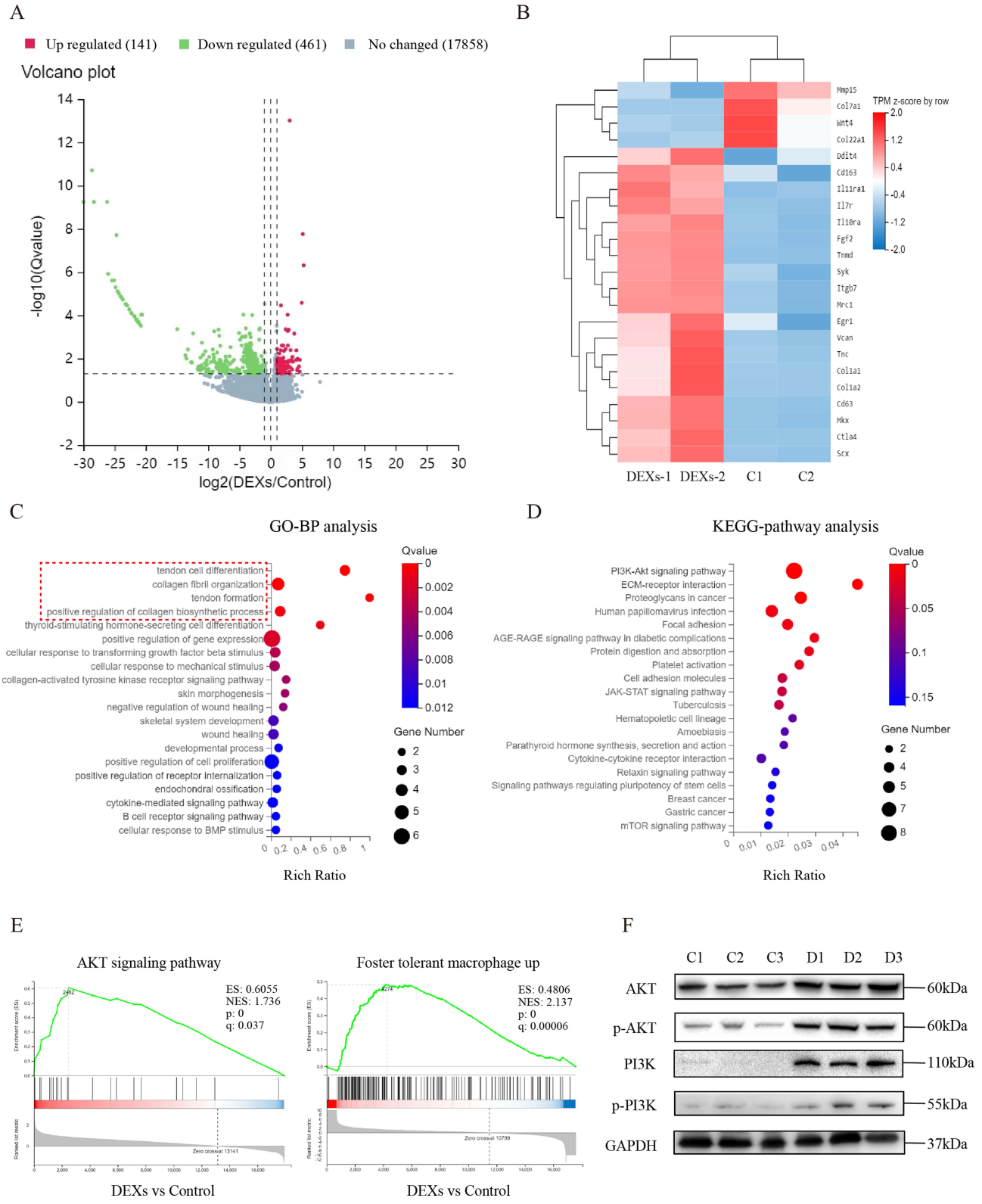

Figure 5 RNA-seq analysis of injured Achilles tendon between PBS and DEXs-treated groups. (**A**) Volcano plot of gene expression (DEXs versus Control; fold change, ≥2; q value < 0.05). (**B**) Heat map of differentiated expression genes. (**C**) GO-BP analysis of differentially expressed genes. (**D**) KEGG analysis of upregulated genes in DEXs treatment group. (**E**) GSEA of the genes associated with AKT signaling and fostering tolerant macrophage. (**F**) WB results showing the protein levels of AKT, p-AKT, PI3K and p-PI3K.

Abbreviations: PBS, phosphate buffered saline; C, control; GO-BP, gene oncology biological process; KEGG, Kyoto Encyclopedia of Genes and Genomes; GSEA, gene set enrichment analysis; NES, normalized enrichment score; FDR, false discovery rate; AKT, threonine kinase A; p-AKT, phosphorylated AKT; PI3K, phosphoinositol 3 kinase; p-PI3K, phosphorylated PI3K.

https://doi.org/10.2147/IJN.S466363 DovePress

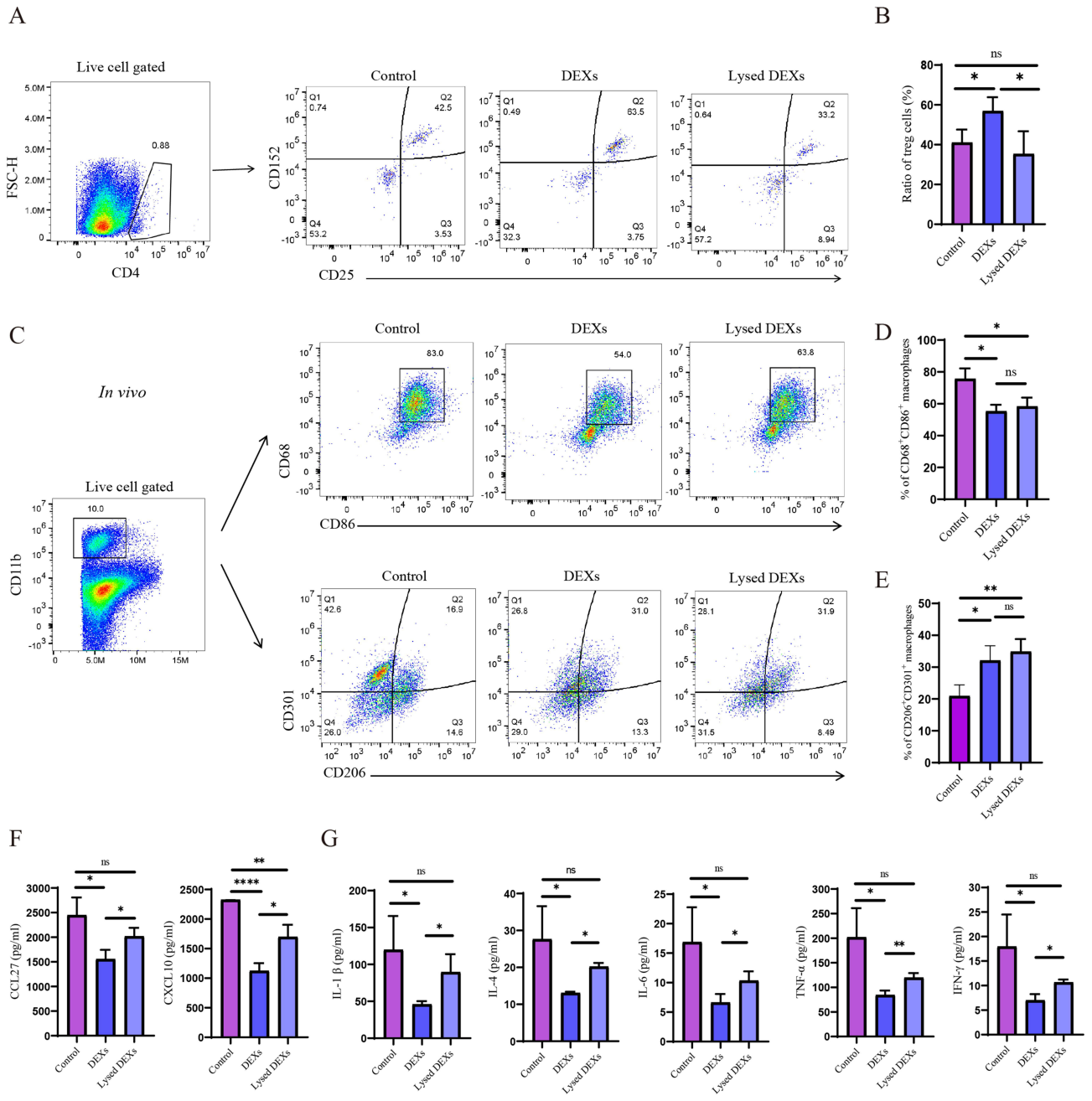

Figure 6 The immunosuppressive function decreased after DEXs were lysed. (**A**) Representative flow cytometry analysis of Tregs collected from injured Achilles tendon between PBS, DEXs or lysed DEXs-treated groups. (**B**) Statistical analysis of the proportions of $CD4^+CD25^+CD152^+$ cells affected H and (**I**) Quantitative results of multiple factors in injured Achilles tendon lysate assessed by Luminex (n=3). (**C**) Representative flow cytometry analysis of macrophages collected from injured Achilles tendon between PBS, DEXs or lysed DEXs-treated groups. (**D** and **E**) Statistical analysis of the proportions of $CD11b^+CD68^+CD86^+$ cells and $CD11b^+CD206^+CD301^+$ cells. (**F** and **G**) Quantitative results of multiple factors in injured Achilles tendon lysate assessed by Luminex (n=3). *P < 0.05, **P < 0.01, ****P < 0.0001.
Abbreviations: TNF-α, tumor necrosis factor-alpha; IFN-γ, interferon-γ.

DEXs Induced the Conversion of M1 Macrophages to M2 Macrophages

LY294002, a specific inhibitor of PI3K/AKT, was injected into our tendinopathy mouse models. In the injured Achilles tendons of DEXs-treated mice, the protein levels of AKT, p-AKT, PI3K, and p-PI3K were found to be partially suppressed by LY294002 (Figure 7A). Additionally, IL-10 expression was detected in the DEXs (Figure 7B). We observed that DEXs upregulated the expression of AKT, PI3K, and IL-10 at the protein level in macrophages, but this effect was inhibited when LY294002 was used to permeabilize the macrophages (Figure 7C). DEXs were also found to

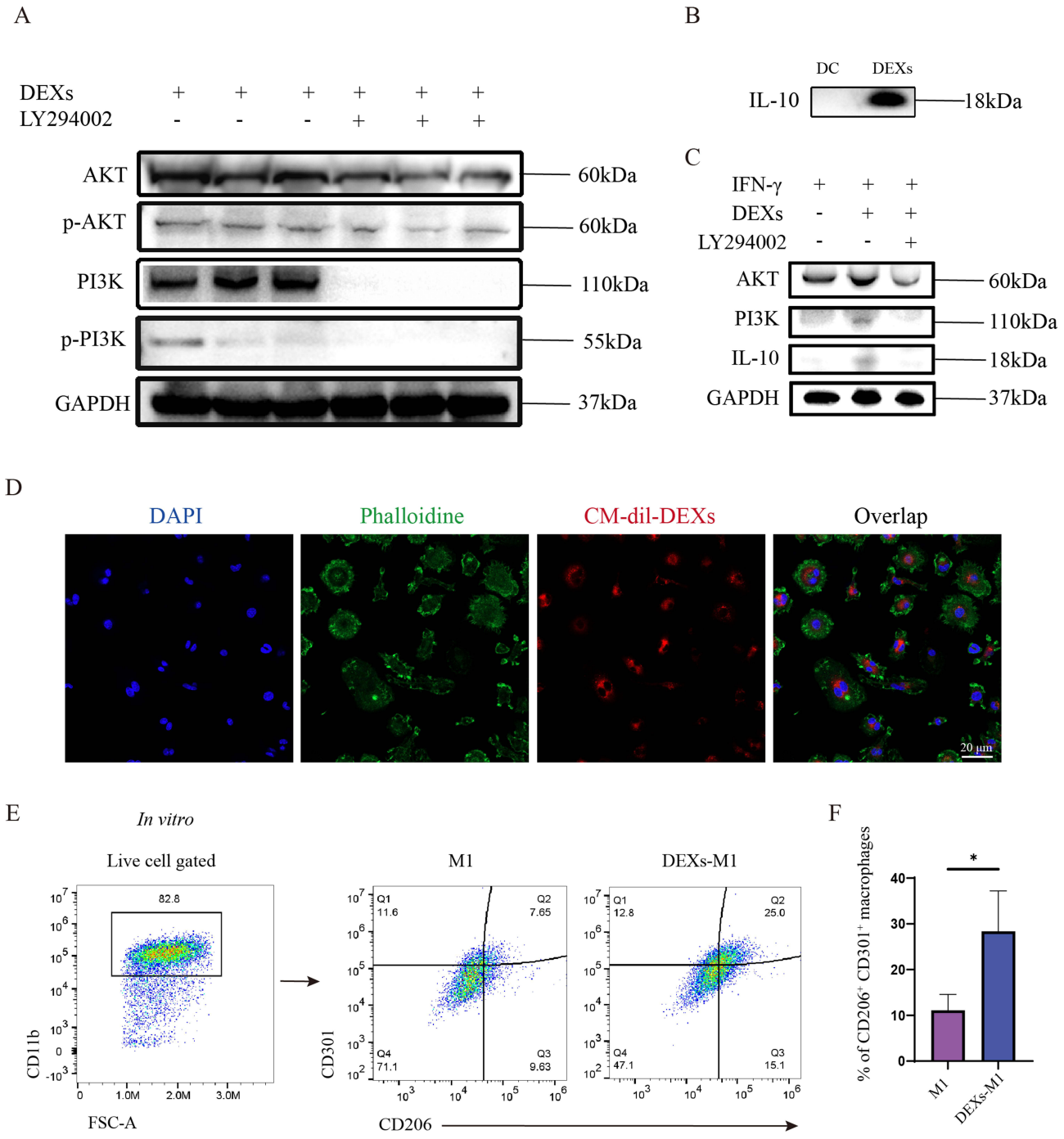

Figure 7 DEXs promote M1 macrophages into M2 polarization. (**A**) WB experiments showing the protein levels of AKT, PI3K and p-PI3K in DEXs-treated groups with or without application of LY294002. (**B**) IL-10 were detected in DEXs using WB. (**C**) WB experiments showing the protein levels of AKT, PI3K, IL-10 and GAPDH expressed by macrophages. (**D**) Investigation of CM-dil-labeled DEXs uptake by M1 macrophages using confocal microscopy. (**E and F**) Representative flow cytometry analysis of the phenotype of macrophages, along with statistical analysis of the proportions of $CD206^{+}CD301^{+}$ cells (n=3). *P < 0.05.

be taken up by M1 macrophages in vitro (Figure 7D), which promoted M2 polarization (Figure 7E and F). In summary, these results indicate that DEXs promote the conversion of M1 macrophages into M2 polarization by activating the PI3K/AKT pathway.

Discussion

Our study demonstrates the pivotal role of DEXs in promoting the repair of tendon injuries by significantly accelerating the synthesis of COLI, facilitating tendon differentiation, alleviating neuropathic pain, and improving the mechanical strength of the tendon. During the acute phase of tendon injury, M1 macrophages infiltrate the injured site, and DEXs can be retained by the injured tendon for several days. This retention induces a shift in macrophages from M1 to M2 via PI3K/AKT signal pathway, thereby improving the local inflammatory microenvironment and leading to decreased levels of inflammatory factors. In summary, DEXs treatment exhibited a favorable therapeutic effect in inhibiting inflammation, promoting tendon healing, and preventing the development of tendinopathy through the PI3K/AKT pathway.

Tendon injuries often progress to tendinopathy without proper repair.[27] Wang et al detected typical manifestations of tendinopathy at POD 7 day in a rat model of collagenase-induced Achilles tendon injury, and showed a gradually worsening trend without treatment. Heterotopic ossification (HO), a subtype of tendinopathy, usually appears 6 weeks after chronic tendon injury, would severely limits tendon movement and ruins tendon function.[28,29] Previous studies have shown that TSPCs in tendinopathy erroneously differentiation into the osteochondro-lineage is one of the pathomechanisms of HO.[12] Our combined in vivo and in vitro experiments, including RNA-seq analysis, revealed that DEXs treatment plays a crucial role in preventing tendon HO by promoting tendon differentiation and downregulating abnormal type of collagen. Moreover, the decrease in matrix metalloproteinase 15 (MMP15) after treatment indicates that DEXs protect the ECM by preventing its degradation, indicating that DEXs may also be used as an effective strategy for treating other diseases associated with collagen degradation.

Inflammation is a natural response to injury and involves the participation of immune cells, particularly pro-inflammatory monocyte-derived macrophages, which play a central role in the development of tendinopathy. In our study, the cytokines released by M1 macrophages, including IL-1β, TNF-α, and IL-6, decreased after DEXs treatment. In contrast, the anti-inflammatory cytokine IL-10, which also serves as an M2 marker,[30] was upregulated after DEXs treatment. Consistent with other studies, these findings confirm that shifting the polarization of infiltrated macrophages is effective in improving the inflammatory microenvironment and preventing tendinopathy.[4] Additionally, Treg cells play a critical role in regulation of differentiation of immune cells, particularly in T-cell-mediated immune responses.[17] Our study demonstrated $CD4^+$ T cells also infiltrated the injured tendons, after DEXs treatment, some of them were induced to differentiate into Treg cells, resulting in downregulated secretion of IL-4 and IFN-γ. This suggests that DEXs induces immune tolerance in tendinopathy.

EXOs have garnered attention in tendinopathy research due to their noninvasive nature and potential to promote tissue repair through the delivery of crucial molecules.[8,31] Additionally, DEXs express CD55 and CD59, which protect them from enzymatic and complement-mediated degradation.[32] When exosomal integrity was compromised, we found that the function of DEXs was greatly reduced, likely due to the impaired delivery of multiple molecules. Treating TSPCs with the inflammatory cytokine IL-1β typically diminished the expression of COLI and tendon markers. However, after DEXs treatment, we detected significantly higher expression of normal collagen and tendon markers, along with a downregulation of COLIII, which may influence fibril stiffness and local mechanics in tendinopathy.[33] Previous studies have highlighted the regenerative abilities of EXOs derived from mesenchymal stem cells (MSCs) in addressing tendinopathy.[22,31,] BMDCs, derived from the differentiation bone marrow mesenchymal stem cells (BMSCs), secrete DEXs, representing one of the major pathways of extracellular signalling.[17] Our results with DEXs demonstrated, for the first time, that DEXs have a strong ability to promote tissue regeneration and regulate inflammation in tendinopathy.

Notably, activation of PI3K/AKT pathway has been shown to restrain pro-inflammatory reactions and promote anti-inflammatory responses in macrophages.[30] To validate the role of the PI3K/AKT pathway in M2 polarization, we examined the expression levels of PI3K/AKT pathway-related proteins after blocking this pathway with PI3K inhibitor LY294002. WB results showed that LY294002 inhibited the upregulation of AKT, p-PI3K and IL-10 induced by DEXs treatment of macrophages. Moreover, the relationship the PI3K/AKT pathway and effect of DEXs on tendinopathy and macrophages polarization was also confirmed in vivo experiments with PI3K inhibitor LY294004, KEGG-pathway analysis and GSEA results.

While our study elucidates the mechanism by which DEXs improve the inflammatory microenvironment in tendinopathy, it also has limitations. The specific constituents of DEXs responsible for stimulating the PI3K/AKT pathway in

M1 macrophages remain not quite unclear. Future research is needed to identify the role of specific miRNAs or proteins in macrophage reprogramming. Additionally, the role of chemokines such as CXCL10 and CCL27 in tendinopathy treatment requires further investigation, preferably using knockout mice in animal experiments. Finally, enhancing the production capacity and targetability of DEXs with biomaterial tools is essential for potential clinical application.

Conclusion

In conclusion, this study demonstrated that DEXs promoted tendon formation, restore normal collagen organization, and improved the biomechanical properties of the injured tendon. These processes may depend on the activation of the PI3K/AKT signaling pathway. Additionally, DEXs exhibited anti-inflammatory effects in tendinopathy by inducing macrophage polarization towards the M2 phenotype and promoting Treg cell differentiation. These results provides significant potential for advancing the tendinopathy treatment approach in the clinic.

Funding

The work was supported by National Natural Science Foundation of China (No. 82072428 and 82300460).

Disclosure

The authors declare that they have no competing interests in this work.

References

1. Ramirez DM, Ramirez MR, Reginato AM, Medici D. Molecular and cellular mechanisms of heterotopic ossification. *Histol Histopathol*. 2014;29(10):1281–1285. doi:10.14670/HH-29.1281
2. Wang X, Xu K, Zhang E, et al. Irreversible electroporation improves tendon healing in a rat model of collagenase-induced achilles tendinopathy. *Am J Sports Med*. 2023;51(7):1831–1843. doi:10.1177/03635465231167860
3. Nourissat G, Berenbaum F, Duprez D. Tendon injury: from biology to tendon repair. *Nat Rev Rheumatol*. 2015;11(4):223–233. doi:10.1038/nrrheum.2015.26
4. Millar NL, Murrell GA, McInnes IB. Inflammatory mechanisms in tendinopathy - towards translation. *Nat Rev Rheumatol*. 2017;13(2):110–122. doi:10.1038/nrrheum.2016.213
5. Ackerman JE, Best KT, Muscat SN, Loiselle AE. Metabolic regulation of tendon inflammation and healing following injury. *Curr Rheumatol Rep*. 2021;23(3):15. doi:10.1007/s11926-021-00981-4
6. Ackermann PW, Hart DA. Metabolic influences on risk for tendon disorders preface. *Adv Exp Med Biol*. 2016;920:V–Vi.
7. Schulze-Tanzil G, Al-Sadi O, Wiegand E, et al. The role of pro-inflammatory and immunoregulatory cytokines in tendon healing and rupture: new insights. *Scand J Med Sci Sports*. 2011;21(3):337–351. doi:10.1111/j.1600-0838.2010.01265.x
8. Chamberlain CS, Kink JA, Wildenauer LA, et al. Exosome-educated macrophages and exosomes differentially improve ligament healing. *Stem Cells*. 2021;39(1):55–61. doi:10.1002/stem.3291
9. Kjaer M, Langberg H, Heinemeier K, et al. From mechanical loading to collagen synthesis, structural changes and function in human tendon. *Scand J Med Sci Sports*. 2009;19(4):500–510. doi:10.1111/j.1600-0838.2009.00986.x
10. Millar NL, Reilly JH, Kerr SC, et al. Hypoxia: a critical regulator of early human tendinopathy. *Ann Rheumatic Dis*. 2012;71(2):302–310. doi:10.1136/ard.2011.154229
11. Magnan B, Bondi M, Pierantoni S, Samaila E. The pathogenesis of Achilles tendinopathy: a systematic review. *Foot Ankle Surg*. 2014;20(3):154–159. doi:10.1016/j.fas.2014.02.010
12. Chen Y, Shen W, Tang C, et al. Targeted pathological collagen delivery of sustained-release rapamycin to prevent heterotopic ossification. *Sci Adv*. 2020;6(18):eaay9526. doi:10.1126/sciadv.aay9526
13. John T, Lodka D, Kohl B, et al. Effect of pro-inflammatory and immunoregulatory cytokines on human tenocytes. *J Orthop Res*. 2010;28(8):1071–1077. doi:10.1002/jor.21079
14. Cui H, He Y, Chen S, Zhang D, Yu Y, Fan C. Macrophage-derived miRNA-containing exosomes induce peritendinous fibrosis after tendon injury through the miR-21-5p/Smad7 pathway. *Mol Ther Nucleic Acids*. 2019;14:114–130. doi:10.1016/j.omtn.2018.11.006
15. Alahdal M, Zhang H, Huang R, et al. Potential efficacy of dendritic cell immunomodulation in the treatment of osteoarthritis. *Rheumatology*. 2021;60(2):507–517. doi:10.1093/rheumatology/keaa745
16. Morelli AE, Bracamonte-Baran W, Burlingham WJ. Donor-derived exosomes: the trick behind the semidirect pathway of allorecognition. *Curr Opin Organ Transplant*. 2017;22(1):46–54. doi:10.1097/MOT.0000000000000372
17. Lee ES, Sul JH, Shin JM, et al. Reactive oxygen species-responsive dendritic cell-derived exosomes for rheumatoid arthritis. *Acta Biomater*. 2021;128:462–473. doi:10.1016/j.actbio.2021.04.026
18. Kim SH, Lechman ER, Bianco N, et al. Exosomes derived from IL-10-treated dendritic cells can suppress inflammation and collagen-induced arthritis. *J Iimmunol*. 2005;174(10):6440–6448. doi:10.4049/jimmunol.174.10.6440
19. Peche H, Renaudin K, Beriou G, Merieau E, Amigorena S, Cuturi MC. Induction of tolerance by exosomes and short-term immunosuppression in a fully MHC-mismatched rat cardiac allograft model. *Am J Transplant*. 2006;6(7):1541–1550. doi:10.1111/j.1600-6143.2006.01344.x
20. Zhang Y, Cai Z, Shen Y, et al. Hydrogel-load exosomes derived from dendritic cells improve cardiac function via Treg cells and the polarization of macrophages following myocardial infarction. *J Nanobiotechnology*. 2021;19(1):271. doi:10.1186/s12951-021-01016-x

21. Thomopoulos S, Parks WC, Rifkin DB, et al. Mechanisms of tendon injury and repair. *J Orthop Res*. 2015;33(6):832–839. doi:10.1002/jor.22806
22. Wang Y, He G, Guo Y, et al. Exosomes from tendon stem cells promote injury tendon healing through balancing synthesis and degradation of the tendon extracellular matrix. *J Cell & Mol Med*. 2019;23(8):5475–5485. doi:10.1111/jcmm.14430
23. Liu RC, Zhou B, Zhang H, et al. Inhibition of ROS activity by controlled release of proanthocyanidins from mesoporous silica nanocomposites effectively ameliorates heterotopic ossification in tendon. *Chem Eng J*. 2021;420.
24. Cui J, Ning LJ, Wu FP, et al. Biomechanically and biochemically functional scaffold for recruitment of endogenous stem cells to promote tendon regeneration. *NPJ Regen Med*. 2022;7(1):26. doi:10.1038/s41536-022-00220-z
25. Andia I, Rubio-Azpeitia E, Maffulli N. Platelet-rich plasma modulates the secretion of inflammatory/angiogenic proteins by inflamed tenocytes. *Clin Orthop Relat Res*. 2015;473(5):1624–1634. doi:10.1007/s11999-015-4179-z
26. Li T, Zhang Z, Bartolacci JG, et al. Graft IL-33 regulates infiltrating macrophages to protect against chronic rejection. *J Clin Invest*. 2020;130 (10):5397–5412. doi:10.1172/JCI133008
27. Feng H, Xing W, Han Y, et al. Tendon-derived cathepsin K-expressing progenitor cells activate hedgehog signaling to drive heterotopic ossification. *J Clin Invest*. 2020;130(12):6354–6365. doi:10.1172/JCI132518
28. Tang Y, Sun Y, Zeng J, et al. Exosomal miR-140-5p inhibits osteogenesis by targeting IGF1R and regulating the mTOR pathway in ossification of the posterior longitudinal ligament. *J Nanobiotechnol*. 2022;20(1):452. doi:10.1186/s12951-022-01655-8
29. Lees-Shepard JB, Goldhamer DJ. Stem cells and heterotopic ossification: lessons from animal models. *Bone*. 2018;109:178–186. doi:10.1016/j.bone.2018.01.029
30. Li L, Jiang W, Yu B, et al. Quercetin improves cerebral ischemia/reperfusion injury by promoting microglia/macrophages M2 polarization via regulating PI3K/Akt/NF-kappaB signaling pathway. *Biomed Pharmacother*. 2023;168:115653. doi:10.1016/j.biopha.2023.115653
31. Liu A, Wang Q, Zhao Z, et al. Nitric oxide nanomotor driving exosomes-loaded microneedles for achilles tendinopathy healing. *ACS nano*. 2021;15 (8):13339–13350. doi:10.1021/acsnano.1c03177
32. Clayton A, Harris CL, Court J, Mason MD, Morgan BP. Antigen-presenting cell exosomes are protected from complement-mediated lysis by expression of CD55 and CD59. *Eur J Immunol*. 2003;33(2):522–531. doi:10.1002/immu.200310028
33. Birch HL. Tendon matrix composition and turnover in relation to functional requirements. *Int J Exp Pathol*. 2007;88(4):241–248. doi:10.1111/j.1365-2613.2007.00552.x